Journal of Catalysis 276 (2010) 181–189

Contents lists available at ScienceDirect

Journal of Catalysis

journal homepage: www.elsevier.com/locate/jcat

Solid acid catalysts based on $H_3PW_{12}O_{40}$ heteropoly acid: Acid and catalytic properties at a gas–solid interface

Ali M. Alsalme, Paul V. Wiper, Yaroslav Z. Khimyak, Elena F. Kozhevnikova, Ivan V. Kozhevnikov *

Department of Chemistry, University of Liverpool, Liverpool L69 7ZD, UK

ARTICLE INFO

Article history:
Received 24 May 2010
Revised 9 September 2010
Accepted 11 September 2010
Available online 14 October 2010

Keywords:
Heterogeneous acid catalysis
Heteropoly acid
Interaction with support
Isopropanol dehydration

ABSTRACT

Solid acid catalysts prepared by supporting 15 wt%$H_3PW_{12}O_{40}$ heteropoly acid (HPA) on TiO_2, ZrO_2 and Nb_2O_5 with a sub-monolayer HPA coverage were characterised at a gas–solid interface, regarding their acid properties and chemical structure of HPA on the catalyst surface and compared to "standard" HPA catalysts such as bulk and silica-supported $H_3PW_{12}O_{40}$ and $Cs_{2.5}H_{0.5}PW_{12}O_{40}$. In contrast to the parent acid, $H_3PW_{12}O_{40}$, possessing strong Brønsted acid sites, the catalysts supported on TiO_2, ZrO_2 and Nb_2O_5 have both Brønsted and Lewis acid sites, with the latter mainly originating from the oxide support. The strength of acid sites in these catalysts is weaker than that in $H_3PW_{12}O_{40}$ and $Cs_{2.5}H_{0.5}PW_{12}O_{40}$. The catalytic activity (turnover frequency) in gas-phase isopropanol dehydration decreases in the order: $H_3PW_{12}O_{40} > Cs_{2.5}H_{0.5}PW_{12}O_{40} > 15\%H_3PW_{12}O_{40}/SiO_2 > 15\%H_3PW_{12}O_{40}/TiO_2 > 15\%H_3PW_{12}O_{40}/Nb_2O_5 > 15\%H_3PW_{12}O_{40}/ZrO_2$, which is in line with the acid strength as determined by NH_3 adsorption calorimetry. Ammonia adsorption calorimetry, $^{31}P\{^1H\}$ MAS NMR and FTIR indicate increasing interaction between support and HPA in the following order of supports: $SiO_2 < TiO_2 < Nb_2O_5 < ZrO_2$.

1. Introduction

Heterogeneous acid catalysis by heteropoly acids (HPAs) has attracted much interest because of its potential to generate economic rewards and green benefits [1–4]. For example, the synthesis of ethyl acetate from acetic acid and ethylene over silica-supported HPA in the gas phase has been commercialised by Showa Denko in Japan [3] and BP in the United Kingdom [5]. The majority of catalytic applications use the most stable and easy available Keggin HPAs comprising heteropoly anions of the formula $[XM_{12}O_{40}]^{n-}$, where X is the heteroatom (P^{5+}, Si^{4+}, etc.) and M the addendum atom (Mo^{6+}, W^{6+}, etc.). HPAs possess stronger acidity than conventional solid acid catalysts such as acidic oxides and zeolites. The acid strength of Keggin HPAs decreases in the order: $H_3PW_{12}O_{40} > H_4SiW_{12}O_{40} > H_3PMo_{12}O_{40} > H_4SiMo_{12}O_{40}$ [1,2]. Usually, tungsten HPAs are the acid catalysts of choice because of their stronger acidity, higher thermal stability and lower oxidation potential compared to molybdenum HPAs [1–4].

The temperature at which Keggin HPAs lose all acidic protons (e.g., $H_3PW_{12}O_{40} \rightarrow PW_{12}O_{38.5} + 1.5\ H_2O$) decreases in the order: $H_3PW_{12}O_{40}$ (465 °C) > $H_4SiW_{12}O_{40}$ (445 °C) > $H_3PMo_{12}O_{40}$ (375 °C) > $H_4SiMo_{12}O_{40}$ (350 °C) [2], the strongest acid $H_3PW_{12}O_{40}$ being the most stable one. Complete decomposition of Keggin structure to the constituent oxides occurs at higher temperatures, but follows the same order: 610, 540, 495 and 375 °C, respectively [6]. Relatively low thermal stability of HPAs and difficulty in catalyst regeneration renders their use in heterogeneous catalysis rather limited [2,4].

The development of HPA catalysts possessing higher thermal stability is an important challenge [4]. In recent years, there has been considerable activity in this direction, focussing mainly on acidic composites comprising tungsten HPAs and Nb_2O_5, ZrO_2 and TiO_2 as oxide matrixes [7–15]. (Work on supported HPA catalysts published before 2000 has been extensively reviewed elsewhere [16]). These composites are usually prepared by wet chemical synthesis, followed by calcination at 500–850 °C, i.e., at temperatures considerably higher than the temperature of HPA decomposition. These materials have been found active in a range of acid-catalysed reactions, often with good catalyst recycling. Only limited knowledge of their acid properties is available, though. Their catalytic activity is often lower than that of the "standard" solid HPA catalysts, such as bulk and silica-supported $H_3PW_{12}O_{40}$ and $Cs_{2.5}H_{0.5}PW_{12}O_{40}$, which indicates weaker acid sites compared to the "standard" HPA catalysts. This, however, can be compensated for by a better performance stability and recyclability of such composites [7–15].

The state of $H_3PW_{12}O_{40}$ on the surface of Nb_2O_5, ZrO_2 and TiO_2 has been studied by various techniques including XRD, FTIR and ^{31}P MAS NMR [7,8,10,12,13,16–18]. Amongst the main factors determining the stability of such catalysts are the calcination temperature, the nature of support and the HPA loading. It has been found that $H_3PW_{12}O_{40}$ that forms in the H_3PO_4–WO_3–Nb_2O_5

* Corresponding author. Fax: +44 151 794 3588.
E-mail address: I.V.Kozhevnikov@liverpool.ac.uk (I.V. Kozhevnikov).

0021-9517/$ - see front matter © 2010 Elsevier Inc. All rights reserved.
doi:10.1016/j.jcat.2010.09.014

system partially decomposes upon calcination at 500 °C. A recent study of 25%$H_3PW_{12}O_{40}/Nb_2O_5$ catalyst has revealed HPA decomposition between 400 and 500 °C, with profound loss of catalyst activity in esterification of fatty acids [17]. In 20%$H_3PW_{12}O_{40}/TiO_2$ calcined at 700 °C, both fragmented and intact HPA species have been found [13]. In $H_3PW_{12}O_{40}/ZrO_2$ calcined at 750 °C, the HPA has been claimed to be stabilised by ZrO_2, unless its loading exceeds a monolayer (15 wt%) [10]. Earlier, however, it had been found that $H_3PW_{12}O_{40}$ on ZrO_2 decomposes above 500 °C [18]. Reportedly, $H_3PW_{12}O_{40}$ is present on the mixed support ZrO_2–MCM-41 even after calcination at 850 °C [12]. This should be treated with caution, however, since these calcination temperatures are higher than the temperature of decomposition of bulk $H_3PW_{12}O_{40}$.

The aim of this work is to study the acidity and catalytic activity of such composites at a gas–solid interface. This is complemented by the characterisation of catalyst texture and chemical environment of HPA on the catalyst surface. The composites under study comprise the strongest Keggin HPA, $H_3PW_{12}O_{40}$, supported at sub-monolayer coverage on Nb_2O_5, ZrO_2 and TiO_2. These are compared with the "standard" bulk and supported HPA catalysts such as $H_3PW_{12}O_{40}$, $H_3PW_{12}O_{40}/SiO_2$ and $Cs_{2.5}H_{0.5}PW_{12}O_{40}$. Isopropanol dehydration is used as a test reaction to characterise the activity of these catalysts at the gas–solid interface.

2. Experimental

2.1. Chemicals and catalysts

The organic and inorganic chemicals were purchased from Aldrich unless stated otherwise and used as supplied without further purification.

The acidic heteropoly salt $Cs_{2.5}H_{0.5}PW_{12}O_{40}$ was prepared according to the literature procedure [19] by adding dropwise the required amount of aqueous solution of caesium carbonate (0.47 M) to aqueous solution of $H_3PW_{12}O_{40}$ (0.75 M) at room temperature with stirring. The precipitate obtained was aged in aqueous mixture for 48 h at room temperature and dried in a rotary evaporator at 45 °C/3 kPa and after that in an oven at 150 °C/0.1 kPa for 1.5 h. The silica-supported catalyst 15%$H_3PW_{12}O_{40}/SiO_2$ was prepared by wet impregnation of Aerosil-300 silica (300 m^2/g surface area) with an aqueous solution of $H_3PW_{12}O_{40}$ [20]. The mixture was stirred overnight at room temperature, followed by drying in a rotary evaporator. Finally, the catalyst was dried at 150 °C/0.1 kPa for 1.5 h. The catalyst 20%$Cs_2HPW_{12}O_{40}/SiO_2$ was prepared using a modification of the two-step procedure [21]. First, Aerosil-300 (4 g) was impregnated with caesium carbonate by stirring with 50 ml of aqueous solution of Cs_2CO_3 (0.104 g, 0.32 mmol) at room temperature for 3 h, followed by drying in an oven at 100 °C overnight and calcination at 300 °C for 3 h in air. In the second step, the silica-supported Cs_2CO_3 was treated with a stoichiometric amount of $H_3PW_{12}O_{40}$ (0.32 mmol) in methanol (50 ml) at room temperature for 24 h, followed by drying, first in an oven at 100 °C overnight, then at 150 °C/0.1 kPa for 1.5 h.

The catalysts comprising $H_3PW_{12}O_{40}$ (15 wt%) supported onto Nb_2O_5, ZrO_2 and TiO_2 were prepared by wet impregnation of these oxides with $H_3PW_{12}O_{40}$ from aqueous solution. The TiO_2 was a Hombikat purchased from Fluka, which, from manufacturer's specification, is a fine-crystalline anatase modification with a surface area $\geqslant$300 m^2/g and a weight loss on drying $\leqslant$10%. The Nb_2O_5 and ZrO_2 were in-house made hydrous oxides (see below). An aqueous solution of $H_3PW_{12}O_{40}$ (1.5 g) was mixed with 8.5 g oxide support to form hydrogel. It was then aged for 24 h at room temperature with stirring, followed by drying in a rotary evaporator. Finally, the catalyst was calcined in air at 300 or 500 °C for 3 h. Hereafter, the calcination temperature is noted in the catalyst formulation as, for example, 15%$H_3PW_{12}O_{40}/Nb_2O_5$-300 and 15%$H_3PW_{12}O_{40}/Nb_2O_5$-500.

Nb_2O_5 was prepared as described in the literature [22]. $NbCl_5$ powder (5 g) was dissolved in 10 ml of ethanol and slowly added to 200 ml of 0.3 M NH_3 aqueous solution to afford a white precipitate of niobic acid $Nb_2O_5{\cdot}nH_2O$. The precipitate was separated using a centrifuge, washed with distilled water until chloride free as tested with $AgNO_3$ and dried in an oven at 100 °C for 3 h. ZrO_2 was prepared by adding dropwise aqueous ammonium hydroxide (25%) to an aqueous solution of $ZrOCl_2$ at room temperature with intense stirring until a pH of 10 was reached. The hydrogel formed was aged at room temperature for 24 h with stirring, and then filtered through a Buchner funnel. The hydrous ZrO_2 thus obtained was washed with distilled water until chloride free ($AgNO_3$). The oxide was dried in an oven at 100 °C for 24 h.

2.2. Techniques

The BET surface area and porosity of catalysts were determined from nitrogen physisorption measured on a Micromeritics ASAP 2000 instrument at −196 °C. Before the measurement, the samples were evacuated at 250 °C for 2 h. Powder X-ray diffraction (XRD) spectra of catalysts were recorded on a PANalytical Xpert diffractometer with a monochromatic Cu Kα radiation (λ = 0.154 nm). XRD patterns were attributed using the JCPDS database. Thermogravimetric analysis (TGA) was carried out on a Perkin-Elmer TGA 7 instrument under nitrogen flow. ICP-AES elemental analysis was carried out on a Spectro Ciros emission spectrometer.

Diffuse reflectance infrared Fourier transform (DRIFT) spectra of catalysts were taken on a Nicolet NEXUS FTIR spectrometer using powdered catalyst mixtures with KBr. The DRIFT spectra of adsorbed pyridine were obtained using the same instrument equipped with a controlled environment chamber (Spectra-Tech Inc., model 0030-101) as described elsewhere [23]. Catalyst samples were diluted with KBr powder (10 wt% in KBr) and pre-treated at 150 °C/0.01 kPa for 1 h. The samples were then exposed to pyridine vapour at room temperature for 1 h, followed by pumping out at 150 °C for 1 h to remove the physisorbed pyridine. Then, the DRIFT spectra of adsorbed pyridine were recorded at room temperature.

$^{31}P\{^1H\}$ MAS (magic angle spinning) NMR spectra were recorded at 9.4 T and 161.9 MHz with an MAS rate of 10 kHz on a Bruker DSX-400 spectrometer with an MAS triple resonance probe-head using zirconia rotors 4 mm in diameter. The ^{31}P $\pi/2$ pulse length was 3.5 μs with a recycle delay of 30 s, and 3000 scans were accumulated. A ^1H TPPM (two-pulse phase modulation) decoupling pulse length of 5.5 μs with radio frequency field strength of 90.9 kHz was used. The position of the ^{31}P resonances is quoted in ppm from external aqueous 85%H_3PO_4.

Differential heats of ammonia adsorption on the catalysts were measured by a pulse method in a flow system using a Setaram TG-DSC 111 differential scanning calorimeter as described previously [23]. Catalyst samples (30–70 mg) were placed in the calorimeter and pre-treated under a flow of helium (30 ml/min) at 300 °C for 1 h. Then, the temperature was lowered to 100 °C under a flow of He. After sample weight stabilisation at 100 °C (about 2 h), the analysis was performed by successive pulses of 0.50 ml of ammonia into the He flow using a loop fitted in a 6-port valve. Sufficient time was allowed after each pulse for adsorption equilibrium to be reached (about 20 min). Weight gain and the corresponding heat of adsorption were recorded, from which the differential adsorption heat was obtained.

2.3. Catalyst testing

The catalysts were tested in isopropanol dehydration in the gas phase, which was carried out under atmospheric pressure in a Pyrex fixed-bed downflow reactor (9 mm internal diameter) fitted with an on-line gas chromatograph (Varian Star 3400 CX instrument with a 30 m × 0.25 mm × 0.25 μm ZB-1701 capillary column and a flame ionisation detector). The temperature in the reactor was controlled by a Eurotherm controller using a thermocouple placed at the top of the catalyst bed. The gas feed contained isopropanol (5.52 kPa partial pressure) in nitrogen obtained by passing nitrogen flow controlled by a Brooks mass flow controller through a saturator, which held liquid isopropanol at 25 °C to maintain the chosen reactant pressure. The gas feed entered the reactor at the top at a flow rate of 20 ml/min. The reactor was packed with 0.100 g catalyst powder (sieved to 45–180 μm). The configuration of catalyst bed was appropriate to allow adequate plug-flow performance. It should be noted that isopropanol dehydration under the chosen conditions was a zero-order reaction (Section 3.2), hence not affected by axial dispersion in a plug-flow reactor [24]. Prior to reaction, the catalysts were pre-treated in situ at 300 °C in a nitrogen flow (20 ml/min) for 1 h. At regular time intervals, the downstream gas flow was analysed by the on-line GC to obtain isopropanol conversion and product selectivity. In light-off tests, the temperature dependent conversion of isopropanol was measured in a temperature range from 80 °C up to the point where 100% conversion was observed. From these results, the temperature of 50% conversion, T_{50}, was obtained and the apparent activation energy of reaction, E_a, was calculated at isopropanol conversion ⩽10%.

3. Results and discussion

3.1. Catalyst characterisation

The supports that were used for preparing the catalysts were of different origin. Nb_2O_5 and ZrO_2 were in-house made freshly precipitated amorphous hydrous oxides, oven-dried at 100 °C. The TiO_2 support was a commercial Hombikat material (from Fluka), fine-crystalline anatase modification with a surface area ⩾300 m^2/g (manufacturer's value). The SiO_2 support, commercial Aerosil-300, is high-purity amorphous silica fumed in a high-temperature flame, consisting of nanosized nonporous spheres, which upon wetting with water form hydrogel, yielding mesoporous silica after drying. The different origin of supports might have an effect on the chemical structure of HPA supported on their surface. In order to level the said differences, the loading of HPA was carried out by wet impregnation with excess of aqueous HPA solution with a long enough ageing time of 24 h. Silica is well known to rehydrate upon treatment with water. Titania is usually quite inert to rehydrate in the bulk, but it still could rehydrate to some extent at the surface. From TGA, water loss upon heating the supports to 700 °C in N_2 flow was Aerosil-300 (~0%) < Hombikat TiO_2 (2%) < hydrous Nb_2O_5 (8%) < hydrous ZrO_2 (12%). Most of the water was lost below 400 °C.

The reason for choosing the HPA loading of 15 wt% was this. On the one hand, such loading is usually sufficient to provide efficient acid catalysis, and on the other hand, it is small enough to ensure sub-monolayer coverage of the catalyst surface with finely dispersed HPA molecules (see below). Our aim was to avoid large HPA crystallites on the catalyst surface, which would rather behave like the bulk HPA, thus making it more difficult to evaluate HPA/support interaction.

The texture of catalysts and supports studied is shown in Table 1. All the catalysts were mesoporous materials with pore diameters of 24–230 Å. Amongst them, silica- and titania-based catalysts possessed larger pores and zirconia-based ones showed smaller pores, with niobia-based catalysts in between. For HPA catalysts supported on Nb_2O_5 and ZrO_2 hydrous oxides, the surface area reduced upon HPA impregnation followed by calcination at 300 °C and reduced further with increasing the calcination temperature from 300 to 500 °C, as expected. The commercial TiO_2 support decreased its surface area dramatically from ~300 to 44 m^2/g upon pre-treatment at 250 °C in vacuum, which implies that the TiO_2 as supplied consisted of very fine particles, in agreement with manufacturer's specification. Supporting HPA on TiO_2 followed by calcination at 300 and 500 °C had only a little effect on the catalyst surface area (41 and 40 m^2/g, respectively). The texture of our bulk $H_3PW_{12}O_{40}$ and $Cs_{2.5}H_{0.5}PW_{12}O_{40}$ was typical of these materials as reported in the literature [19,25].

Table 1
Catalyst texture from nitrogen adsorption.[a]

Catalyst	S_{BET}[b] (m^2/g)	Pore diameter[c] (Å)	Pore volume[d] (cm^3/g)
SiO_2 (Aerosil-300)	300[e]		
Nb_2O_5-250[a]	287	46	0.33
ZrO_2-250[a]	162	23	0.09
TiO_2	⩾300[e]		
TiO_2-250[a]	44	90	0.10
$H_3PW_{12}O_{40}$-250[a]	2.0	81	0.04
15%$H_3PW_{12}O_{40}/SiO_2$-250[a]	229	204	1.17
15%$H_3PW_{12}O_{40}/Nb_2O_5$-300	166	52	0.22
15%$H_3PW_{12}O_{40}/Nb_2O_5$-500	96	80	0.19
15%$H_3PW_{12}O_{40}/ZrO_2$-300	121	24	0.07
15%$H_3PW_{12}O_{40}/ZrO_2$-500	54	56	0.08
15%$H_3PW_{12}O_{40}/TiO_2$-300	41	154	0.16
15%$H_3PW_{12}O_{40}/TiO_2$-500	40	230	0.23
$Cs_{2.5}H_{0.5}PW_{12}O_{40}$-250[a]	111	24	0.07
20%$Cs_2HPW_{12}O_{40}/SiO_2$-250[a]	185	191	0.88

[a] Prior to N_2 adsorption, the catalysts were pre-treated at 250 °C in vacuum for 2 h.
[b] BET surface area.
[c] Average BET pore diameter.
[d] Single-point total pore volume.
[e] The value of surface area given by manufacturer.

The surface areas of the supported HPA catalysts ranged from 40 to 229 m^2/g. Assuming a cross section of 144 $Å^2$ for the $H_3PW_{12}O_{40}$ molecule [1,2], the 15%HPA loading will correspond to 45 m^2/g monolayer HPA coverage. Therefore, these catalysts could be adequately viewed as having sub-monolayer HPA coverage, with some reservation in case of titania-supported catalysts that had a surface area of 40–41 m^2/g. The XRD spectra (Fig. 1) confirm fine dispersion of HPA on the catalyst surface.

Fig. 1 shows XRD patterns for bulk and supported $H_3PW_{12}O_{40}$ catalysts as well as for catalyst supports. The 15%$H_3PW_{12}O_{40}/Nb_2O_5$ and 15%$H_3PW_{12}O_{40}/ZrO_2$ catalysts, prepared from the amorphous Nb_2O_5 and ZrO_2 hydrous oxides, after calcination at 300 °C were XRD amorphous. After calcination at 500 °C, both the supports and the catalysts became crystalline. Nb_2O_5-500 and 15%$H_3PW_{12}O_{40}/Nb_2O_5$-500 exhibited the pattern of hexagonal niobia. ZrO_2-500 showed the pattern of the tetragonal phase, with a little of monoclinic ZrO_2 also present. 15%$H_3PW_{12}O_{40}/ZrO_2$-500 consisted of a mixture of tetragonal and monoclinic modifications of ZrO_2, the content of monoclinic phase increased compared to the pure ZrO_2-500. 15%$H_3PW_{12}O_{40}/TiO_2$, prepared from commercial anatase TiO_2, also exhibited the pattern of anatase after calcination at 300 and 500 °C. All supported catalysts were XRD amorphous with regard to $H_3PW_{12}O_{40}$, which indicates fine dispersion of HPA on the catalyst surface. XRD pattern of WO_3 was not observed in the catalyst samples. It should be noted that WO_3 has been found in supported HPA catalysts with higher HPA loadings (e.g. 25%$H_3PW_{12}O_{40}/Nb_2O_5$ [17]) after calcination at 500 °C.

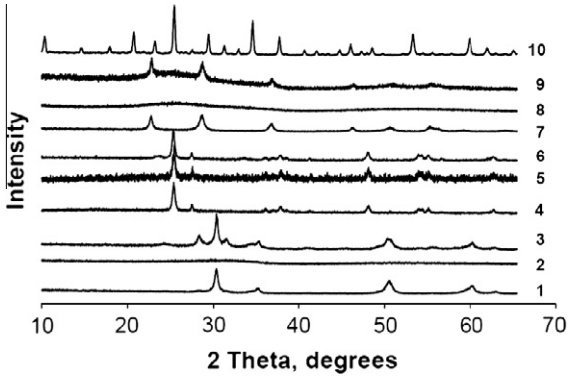

Fig. 1. XRD patterns (Cu Kα radiation) for: (1) ZrO_2-500, (2) 15%$H_3PW_{12}O_{40}/ZrO_2$-300, (3) 15%$H_3PW_{12}O_{40}/ZrO_2$-500, (4) TiO_2-500, (5) 15%$H_3PW_{12}O_{40}/TiO_2$-300, (6) 15%$H_3PW_{12}O_{40}/TiO_2$-500, (7) Nb_2O_5-500, (8) 15%$H_3PW_{12}O_{40}/Nb_2O_5$-300, (9) 15%$H_3PW_{12}O_{40}/Nb_2O_5$-500 and (10) $H_3PW_{12}O_{40}$.

Bulk $H_3PW_{12}O_{40}$ and $Cs_{2.5}H_{0.5}PW_{12}O_{40}$ pre-treated at temperatures below 300 °C are known to possess strong Brønsted acid sites [1,2]. From the DRIFT spectra of adsorbed pyridine (Figs. 2–4), the HPA catalysts supported on Nb_2O_5, ZrO_2 and TiO_2 possessed both Brønsted and Lewis acid sites, as evidenced by strong IR bands at 1540 and 1450 cm^{-1}, respectively. This is consistent with the previous studies of these catalysts [7,10,12,13]. In agreement with the literature [26], the pure oxides Nb_2O_5, ZrO_2 and TiO_2 all exhibited Lewis acid sites. Nb_2O_5 and ZrO_2 also displayed Brønsted acid sites capable of protonating pyridine (Figs. 2–4). Table 2 shows the relative number of Brønsted and Lewis acid sites, B/L, in the catalysts and supports defined as a ratio of areas of DRIFTS peaks at 1540 cm^{-1} and 1450 cm^{-1}. The ratio of extinction coefficients for these peaks has been found close to unity [27]. As expected, the B/L value was higher in supported HPA catalysts than in the corresponding oxide supports. This is more evident for the titania-supported catalysts due to the lack of intrinsic Brønsted acidity in TiO_2. The Nb_2O_5 and ZrO_2 catalysts show smaller increases in B/L values because these supports themselves possess substantial Brønsted acidity. The relative number of Brønsted acid sites decreased with increasing calcination temperature due to catalyst dehydration. In ZrO_2, however, the relative number of Brønsted sites capable of protonating pyridine increased with increasing the calcination temperature from 300 to 500 °C. This may be related to the transformation of ZrO_2 into the tetragonal phase upon calcination (Fig. 1), which has been found to be a more active catalyst in alkane isomerisation (hence probably more acidic) than the monoclinic phase [28]. From the DRIFTS results, it can be concluded that Lewis acid sites in our HPA/Nb_2O_5, HPA/ZrO_2 and HPA/TiO_2 catalysts were mainly originated from the oxide supports, and Brønsted acid sites were provided by the HPA and support (in the case of Nb_2O_5 and ZrO_2).

The strength of acid sites in the catalysts was characterised by measuring the enthalpy of ammonia adsorption at the gas–solid interface. This technique does not discriminate Brønsted and Lewis acid sites. As an example, Fig. 5 shows the determination of the initial enthalpy of NH_3 adsorption, ΔH_i, for $H_3PW_{12}O_{40}$, $Cs_{2.5}H_{0.5}PW_{12}O_{40}$ and 15%$H_3PW_{12}O_{40}/ZrO_2$-500. The ΔH_i values for $H_3PW_{12}O_{40}$ and

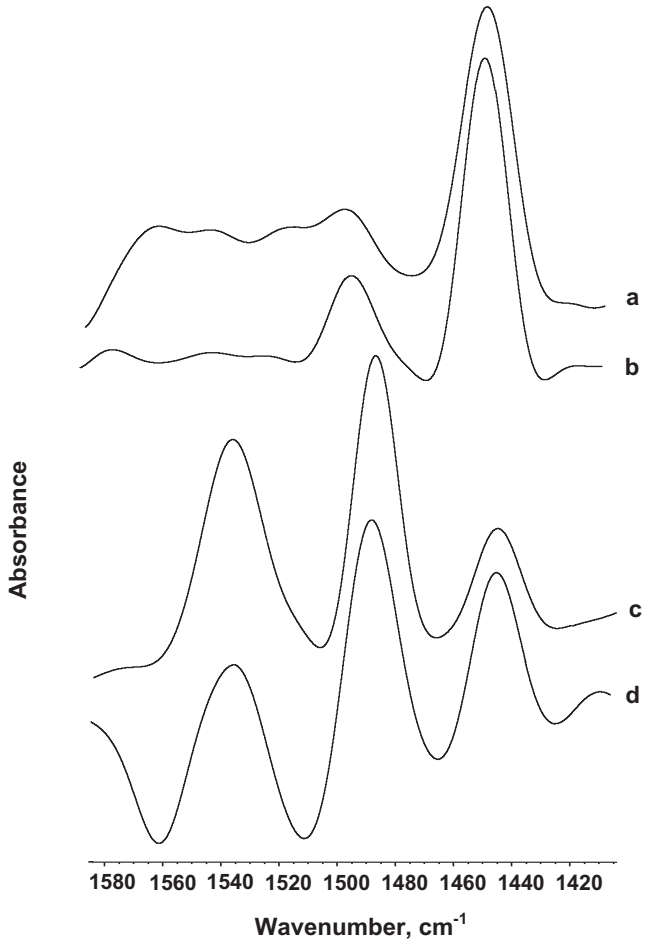

Fig. 2. DRIFT spectra of pyridine adsorbed on (a) TiO_2-300, (b) TiO_2-500, (c) 15%$H_3PW_{12}O_{40}/TiO_2$-300 and (d) 15%$H_3PW_{12}O_{40}/TiO_2$-500.

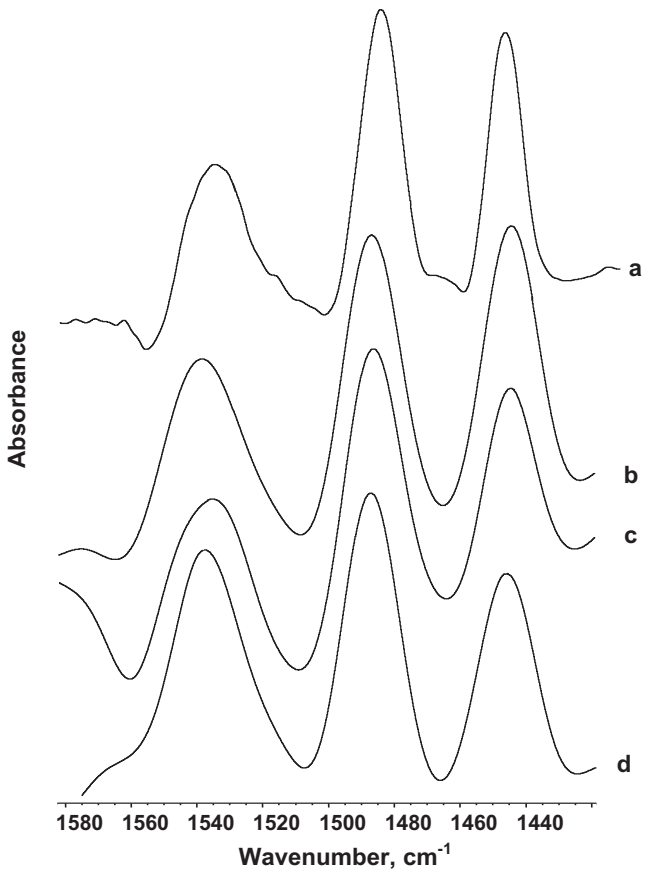

Fig. 3. DRIFT spectra of pyridine adsorbed on (a) Nb_2O_5-300, (b) Nb_2O_5-500, (c) 15%$H_3PW_{12}O_{40}/Nb_2O_5$-300 and (d) 15%$H_3PW_{12}O_{40}/Nb_2O_5$-500.

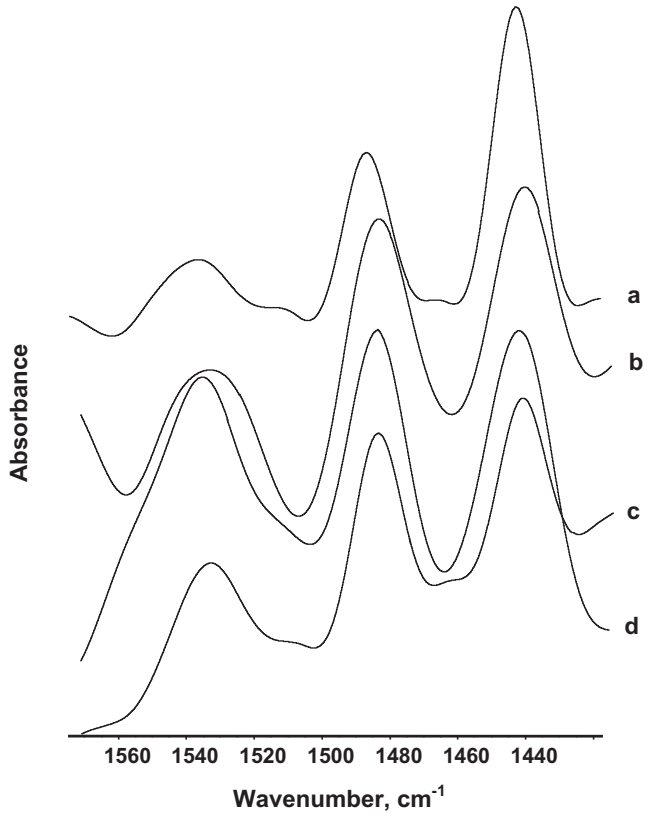

Fig. 4. DRIFT spectra of pyridine adsorbed on (a) ZrO_2-300, (b) ZrO_2-500, (c) 15%$H_3PW_{12}O_{40}/ZrO_2$-300 and (d) 15%$H_3PW_{12}O_{40}/ZrO_2$-500.

$Cs_{2.5}H_{0.5}PW_{12}O_{40}$ are in excellent agreement with those reported previously [29,30]. The values of ΔH_i for all the catalysts under study are given in Table 3. For the catalysts pre-treated at 300 °C, the acid strength decreases in the order: $H_3PW_{12}O_{40}$ > $Cs_{2.5}H_{0.5}PW_{12}O_{40}$ > 20%$Cs_2HPW_{12}O_{40}/SiO_2$ > 15%$H_3PW_{12}O_{40}/SiO_2$ > 15%$H_3PW_{12}O_{40}/TiO_2$ > 15%$H_3PW_{12}O_{40}/Nb_2O_5$ > 15%$H_3PW_{12}O_{40}/ZrO_2$. This shows that the catalysts comprising HPA supported on Nb_2O_5, ZrO_2 and TiO_2 possess weaker acid sites than the "standard" HPA catalysts. Their ΔH_i values are in the range from −121 to −143 kJ/mol, which is similar to those for acidic zeolites [31]. The catalyst acid strength decreases in the order of supports: SiO_2 > TiO_2 > Nb_2O_5 > ZrO_2, which indicates increasing interaction between the HPA and oxide support in that order. This is also confirmed by infrared spectroscopy and ^{31}P NMR (see below).

We examined the state of HPA on Nb_2O_5, ZrO_2 and TiO_2 in comparison with that on SiO_2 by infrared spectroscopy (DRIFTS). The spectra were measured using 10% catalyst mixtures with KBr. All samples contained the same amount of HPA and support. Fig. 6 displays the DRIFT spectra in the range of 750–1150 cm^{-1} characteristic of the Keggin structure. A 15:85 w/w mechanical mixture of bulk HPA and ZrO_2 (both calcined separately at 300 °C in air prior to mixing) exhibits the well-known spectrum of $H_3PW_{12}O_{40}$ (a), with strong bands of stretching vibrations at 1080 (P—O), 983 (terminal W=O group), 890 and 812 cm^{-1} (edge- and corner-sharing W—O—W groups) [1,16]. This spectrum shows that the HPA was not affected by ZrO_2 in this sample, as expected. Spectra (b)–(d), (h) represent supported HPA catalysts calcined at 300 °C and (e)–(g) those calcined at 500 °C. Some of them clearly show the presence of Keggin bands. But their intensity is much weaker compared to those in spectrum (a), despite the same concentration of HPA in all these samples. This can be explained by restriction of molecular vibrations and loss of symmetry in adsorbed HPA species. It is also evident that the nature of support and the calcination temperature play an important role. DRIFT spectra (e)–(g) for HPA supported on Nb_2O_5, ZrO_2 and TiO_2 after calcination at 500 °C show no Keggin unit bands, the spectra being similar to those for the pure oxide supports. This could be the result of HPA decomposition. The catalysts calcined at 300 °C may be expected to be more stable. Indeed, the 15%HPA/TiO_2-300 catalyst exhibits the Keggin bands at 1080 (P—O) and 983 cm^{-1} (W=O) (spectrum (b)). However, no bands of the bridging W—O—W groups appear in this spectrum. In contrast, HPA/ZrO_2-300 and HPA/Nb_2O_5-300 hardly show any Keggin unit bands (spectra (c), (d)) probably due to strong HPA/support interaction leading to partial decomposition of the Keggin unit (see $^{31}P\{^1H\}$ MAS NMR spectra below). The "standard" $H_3PW_{12}O_{40}/SiO_2$ catalyst is known to be stable at 300 °C and beyond, with weak HPA/support interaction [1,2,6,16]. In spectrum (h) for 15%HPA/SiO_2-300, silica exhibits strong infrared bands at 1100 and 806 cm^{-1} and a weak shoulder band at 984 cm^{-1}. The strong bands from silica mask the HPA bands at 1080 and 812 cm^{-1}, but the vibrations at 983 (W=O) and 890 (W—O—W) appear at their normal positions with unchanged relative intensity. From these results, it can be inferred that the HPA/support interaction increases in the series: SiO_2 < TiO_2 < Nb_2O_5, ZrO_2. This is the same order in which the acid strength of the corresponding supported HPA catalysts decreases (Table 3). However, the uncertainty in interpretation of DRIFTS for strongly adsorbed HPA molecules makes it difficult to prove decomposition of supported HPA at

Table 2
Brønsted (*B*) versus Lewis (*L*) acidity of catalysts from DRIFTS of adsorbed pyridine.

Catalyst	B/L^a
TiO_2-300	0.04
TiO_2-500	0.04
15%$H_3PW_{12}O_{40}/TiO_2$-300	2.82
15%$H_3PW_{12}O_{40}/TiO_2$-500	1.53
Nb_2O_5-300	1.32
Nb_2O_5-500	0.99
15%$H_3PW_{12}O_{40}/Nb_2O_5$-300	1.42
15%$H_3PW_{12}O_{40}/Nb_2O_5$-500	1.25
ZrO_2-300	0.32
ZrO_2-500	0.98
15%$H_3PW_{12}O_{40}/ZrO_2$-300	1.42
15%$H_3PW_{12}O_{40}/ZrO_2$-500	1.07

[a] The ratio of intensities (integrals of peak areas) of the DRIFTS peaks at 1540 cm^{-1} and 1450 cm^{-1}.

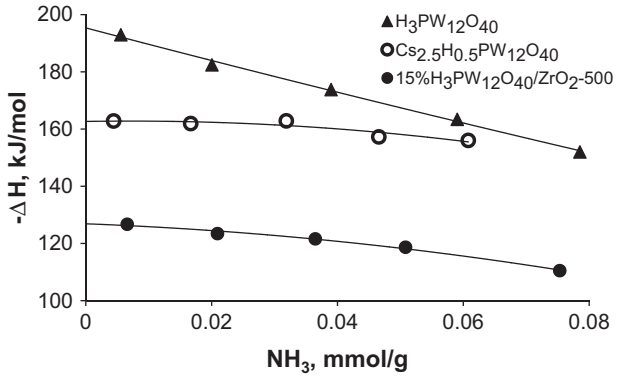

Fig. 5. Enthalpy of NH_3 adsorption versus NH_3 uptake at 100 °C for 15%$H_3PW_{12}O_{40}/ZrO_2$-500, $C_{2.5}H_{0.5}PW_{12}O_{40}$ and $H_3PW_{12}O_{40}$.

Table 3
Isopropanol dehydration.[a]

	Catalyst	T_{50}[b] (°C)	E_a[c] (kJ/mol)	X[d] (%)	TOF[e] (h^{-1})	S[f] (mol%)	$-\Delta H_i$[g] (kJ/mol)
1	$H_3PW_{12}O_{40}$-300	104	90	81	3500[h]	98 (93)	195
2	$Cs_{2.5}H_{0.5}PW_{12}O_{40}$-300	100	68	94	430[h]	99 (91)	164
3	20%$Cs_2H_1PW_{12}O_{40}/SiO_2$-300	105	67	94	430	99 (92)	160
4	15%$H_3PW_{12}O_{40}/SiO_2$-300	103	86	99	190	99 (94)	154
5	15%$H_3PW_{12}O_{40}/TiO_2$-300	110	90	67	130	92 (91)	143
6	15%$H_3PW_{12}O_{40}/TiO_2$-500	137	81	19	36	83 (89)	130
7	15%$H_3PW_{12}O_{40}/Nb_2O_5$-300	155	71	9	17	83 (92)	132
8	15%$H_3PW_{12}O_{40}/Nb_2O_5$-500	165	72	4	8	84 (96)	121
9	15%$H_3PW_{12}O_{40}/ZrO_2$-300	168	59	5	10	(98)	121
10	15%$H_3PW_{12}O_{40}/ZrO_2$-500	170	63	2	4	(92)	127
11	Nb_2O_5-500	200	64	1		(99)	
12	ZrO_2-500	310	43	0		(100)	
13	TiO_2-500	285	41	0		(100)	

[a] Reaction conditions: 0.1 g catalyst, 5.52 kPa isopropanol partial pressure in N_2, 20 ml/min flow rate (2.95 mmol/h rate of isopropanol supply); prior to reaction the catalysts were pre-treated in situ at 300 °C for 1 h in N_2 (20 ml/min).
[b] Temperature corresponding to 50% isopropanol conversion from light-off tests.
[c] Apparent activation energy determined from light-off tests at isopropanol conversion ⩽10%.
[d] Isopropanol conversion at 120 °C.
[e] Turnover frequency per HPA proton site calculated from isopropanol conversion at 120 °C and 2-h time on stream, assuming that all HPA protons were equally available for reaction.
[f] Propene selectivity at 120 °C and in brackets at T_{50}; the only other product was diisopropyl ether.
[g] Initial enthalpy of ammonia adsorption at 100 °C.
[h] Turnover frequency per surface proton site estimated assuming a Keggin anion cross section of 144 Å^2 and using the surface area for fresh catalysts (Table 1).

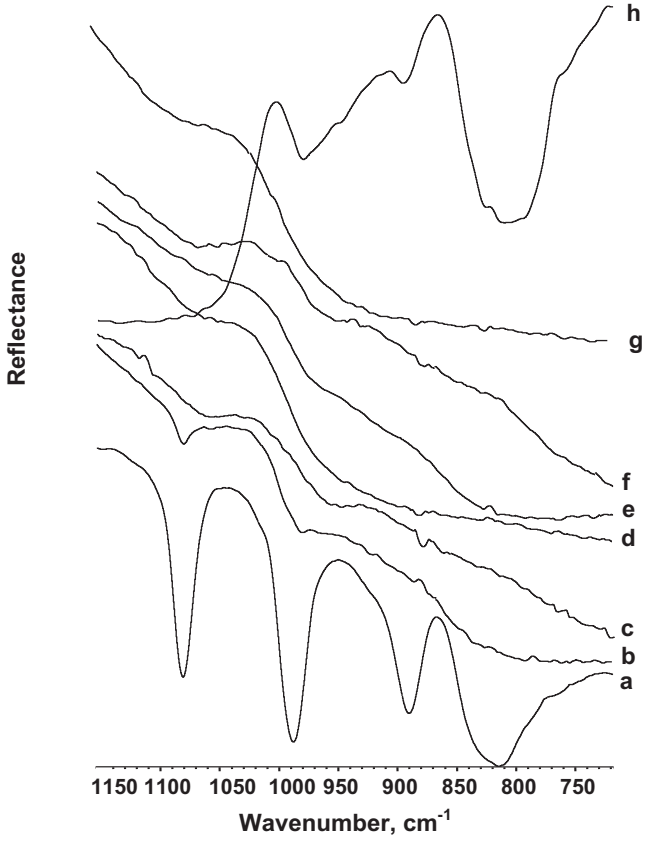

Fig. 6. DRIFT spectra of (a) 15:85 w/w mechanical mixture of $H_3PW_{12}O_{40}$ and ZrO_2 (calcined separately at 300 °C in air, prior to mixing), (b) 15%$H_3PW_{12}O_{40}/TiO_2$-300, (c) 15%$H_3PW_{12}O_{40}/ZrO_2$-300, (d) 15%$H_3PW_{12}O_{40}/Nb_2O_5$-300, (e) 15%$H_3PW_{12}O_{40}/TiO_2$-500, (f) 15%$H_3PW_{12}O_{40}/ZrO_2$-500, (g) 15%$H_3PW_{12}O_{40}/Nb_2O_5$-500 and (h) 15%$H_3PW_{12}O_{40}/SiO_2$-300.

sub-monolayer coverage, i.e., the absence of HPA bands does not prove HPA decomposition.

Further insight into the state of HPA in the catalysts under study can be gained by ^{31}P solid-state NMR. Fig. 7 shows the $^{31}P\{^1H\}$ MAS NMR spectra for bulk and supported $H_3PW_{12}O_{40}$ catalysts pre-treated at 300 and 500 °C for 3 h in air. The well-documented bulk and SiO_2-supported HPA can be considered as reference systems for the assessment of the state of HPA in supported catalysts. The bulk HPA calcined at 300 °C, which should retain the Keggin structure, indeed exhibits a sharp resonance at −15.3 ppm characteristic of the $H_3PW_{12}O_{40}$ Keggin unit [1,2]. However, some decomposition of the HPA could be noted (peaks at −3.7 and −11.5 ppm), which was probably due to a relatively long pre-treatment time (3 h). Predictably, the bulk HPA calcined at 500 °C shows no resonance at *ca.* −15 ppm, which points to partial decomposition of the Keggin structure. The stability of silica-supported HPA calcined at 300 °C is confirmed by the strong peak of the Keggin unit at −15.7 ppm, with some decomposition fragments also present similarly to the bulk HPA (peaks at −11.7 and 3.1 ppm).

The HPA catalysts supported on TiO_2, ZrO_2 and Nb_2O_5 showed different ^{31}P environments. Only the HPA/TiO_2-300 catalyst, calcined at 300 °C, exhibited the presence of a small number of Keggin species (peak at −14.9 ppm). This is in agreement with the DRIFT spectrum (Fig. 6). HPA/TiO_2-300 and HPA/TiO_2-500 display a very broad upfield line centred at about −7.7 ppm, except no Keggin species could be seen in for the latter material. Neither HPA/ZrO_2 nor HPA/Nb_2O_5 exhibited any Keggin species in their $^{31}P\{^1H\}$ MAS NMR spectra, which are also very broad.

Although it is difficult to attribute these ^{31}P NMR spectra to any particular species, the overall situation regarding the state of HPA on the surface of TiO_2, Nb_2O_5 and ZrO_2 appears to be clear. The broad lines probably indicate strong interaction between finely dispersed amorphous HPA species and support leading to partial decomposition of the $PW_{12}O_{40}^{3-}$ anion. There are no intact Keggin species present on Nb_2O_5 and ZrO_2 characteristic of the bulk $H_3PW_{12}O_{40}$. The titania catalyst calcined at 300 °C exhibits some intact Keggin species, which disappear after calcination at 500 °C. The catalysts calcined at 300 and 500 °C contain a number of decomposition fragments represented by the ^{31}P NMR peaks at 2.7–3.1 ppm and −7.6 to −12.5 ppm. The origin of the former is not clear; the latter, on the basis of solution ^{31}P NMR spectra [32], may be assigned to unsaturated tungstophosphate polyoxometalates with atomic ratios W/P < 12, which would imply partial decomposition of the Keggin species to form less acidic tungsto-

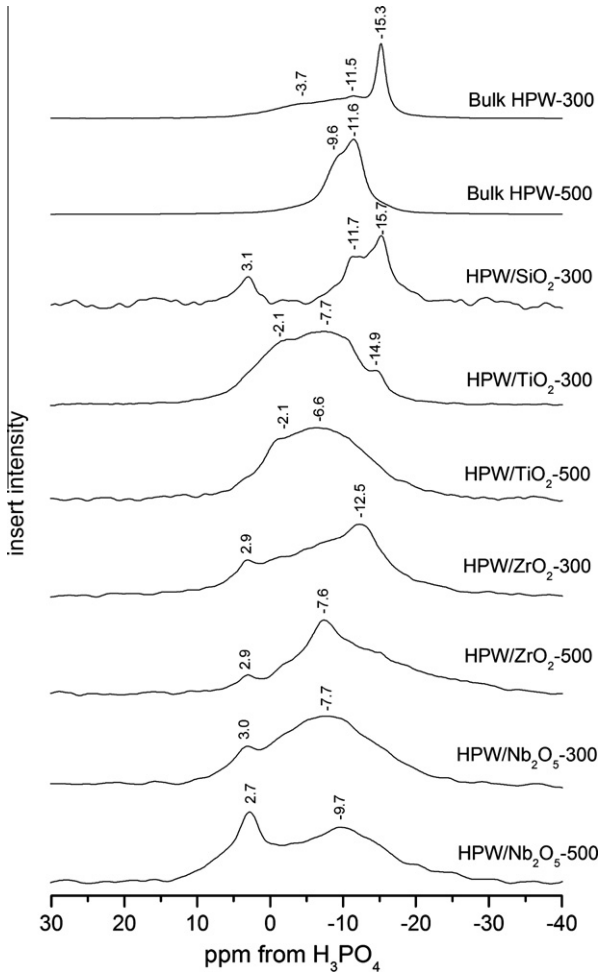

Fig. 7. $^{31}P\{^1H\}$ MAS NMR spectra of catalysts calcined at 300 °C or 500 °C for 3 h in air (HPW stands for $H_3PW_{12}O_{40}$).

phosphates. Unsaturated tungstophosphates have been suggested to form in supported $H_3PW_{12}O_{40}$ catalysts previously [33].

In summary, ^{31}P NMR spectroscopy and DRIFT spectroscopy together with NH_3 adsorption calorimetry indicate that HPA/support interaction increases in the series of supports: $SiO_2 < TiO_2 < Nb_2O_5 < ZrO_2$, decreasing the acid strength of supported HPA catalysts in that order (Table 3). Supported HPA undergoes partial decomposition, as evidenced by ^{31}P NMR (Fig. 7). The degree of decomposition appears to increase in the same order of supports, in line with the relative Brønsted/Lewis acidity, *B*/*L*, of catalysts, which is largely associated with the presence of HPA on the catalyst surface. For the HPA catalysts calcined at 500 °C, the *B*/*L* values decrease in the series $TiO_2 > Nb_2O_5 > ZrO_2$, approaching those for the corresponding supports (Table 2). Amongst the supports studied, silica stands out as the inert support for HPA catalysts, in agreement with previous results.

3.2. Isopropanol dehydration

The dehydration of isopropanol has been widely used for probing the acidity of catalysts through their catalytic activity [26]. Besides water, this reaction yields propene and diisopropyl ether (Eq. (1)). Propene forms in an uphill process, whereas the ether in a downhill process, with standard reaction enthalpies of 50.8 and −15.8 kJ/mol, respectively, for the gas-phase dehydration. On many oxide catalysts, propene is the major reaction product and forms with higher activation energy than the ether [34].

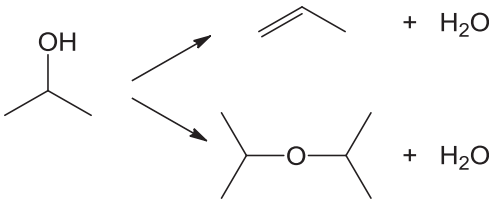

(1)

With catalysts possessing sufficiently strong proton sites, isopropanol dehydration occurs *via* the carbenium ion mechanism ([34] and references therein), and its rate correlates directly with the catalyst acidity (the number and the strength of acid sites). Isopropanol dehydration does not discriminate Brønsted and Lewis acid sites. Lewis acid sites may be affected by the water produced in the reaction, turning into Brønsted acid sites. Gas-phase isopropanol dehydration has been found zero-order in isopropanol over a wide range of oxide catalysts (0.6–2.8 kPa isopropanol partial pressure, 120–300 °C) [34], which indicates full coverage of the catalyst surface with adsorbed alcohol molecules. Bulk and supported $H_3PW_{12}O_{40}$ have been tested in the dehydration of isopropanol as well as other alcohols [1,18,35]. A thorough study of kinetics and mechanism of 2-butanol dehydration over supported HPA catalysts has been published recently [36].

Table 3 shows our results on catalyst activity in isopropanol dehydration. Typically, the reaction reached steady state in less than 15 min and proceeded without catalyst deactivation for at least 4 h on stream. With all catalysts, propene was the major reaction product in the temperature range studied. At the isopropanol partial pressure of 5.52 kPa that was applied in this study, the reaction is likely to be zero-order in isopropanol, as can be inferred from the previous results [34]. This would imply the reaction rates (isopropanol conversions) to be equivalent to the rate constants.

First, the activity of catalysts was characterised per unit catalyst weight by measuring the temperatures of 50% conversion, T_{50}, in light-off tests. An example of such test for $15\%H_3PW_{12}O_{40}/TiO_2$-500 is shown in Fig. 8. The light-off tests rank the catalyst activity by the values of T_{50} as follows: $H_3PW_{12}O_{40} \approx Cs_{2.5}H_{0.5}PW_{12}O_{40} \approx 15\%H_3PW_{12}O_{40}/SiO_2 \approx 20\%Cs_2HPW_{12}O_{40}/SiO_2 > 15\%H_3PW_{12}O_{40}/TiO_2 > 15\%H_3PW_{12}O_{40}/Nb_2O_5 > 15\%H_3PW_{12}O_{40}/ZrO_2 > Nb_2O_5 \gg TiO_2 > ZrO_2$ (Table 3). This order is in agreement with the order of catalyst acid strength determined by NH_3 adsorption calorimetry (Table 3). The "standard" HPA catalysts possess higher activity per catalyst weight than the catalysts comprising HPA supported on Nb_2O_5, ZrO_2 and TiO_2, which is in line with the catalyst acid strength. As expected, supported HPA catalysts are much more active than the corresponding oxide supports, so the supports make only minor (Nb_2O_5) or no contribution (ZrO_2 and TiO_2) to the activity of these catalysts. The activity of supported catalysts decreases with increasing calcination temperature from 300 to 500 °C, in accord with the catalyst acid strength. This can be explained by the loss of proton sites due to catalyst dehydration and the decrease in surface area (Table 1).

The apparent activation energies, E_a, for HPA catalysts estimated from isopropanol conversion ($\leqslant$10%) in the light-off tests were in the range of 59–90 kJ/mol (Table 3). These can be regarded almost equal to the true activation energies given the reaction being zero-order in isopropanol (see above). The E_a values obtained suggest that the reaction with all the catalysts studied occurred in the chemical regime without diffusion limitations. Although any discussion of individual E_a values is hardly possible at this stage, it is worth noting that the E_a values for HPA catalysts are significantly lower than those for Al_2O_3, SiO_2 and MgO oxide catalysts [34], as expected from the acid strength of these catalysts.

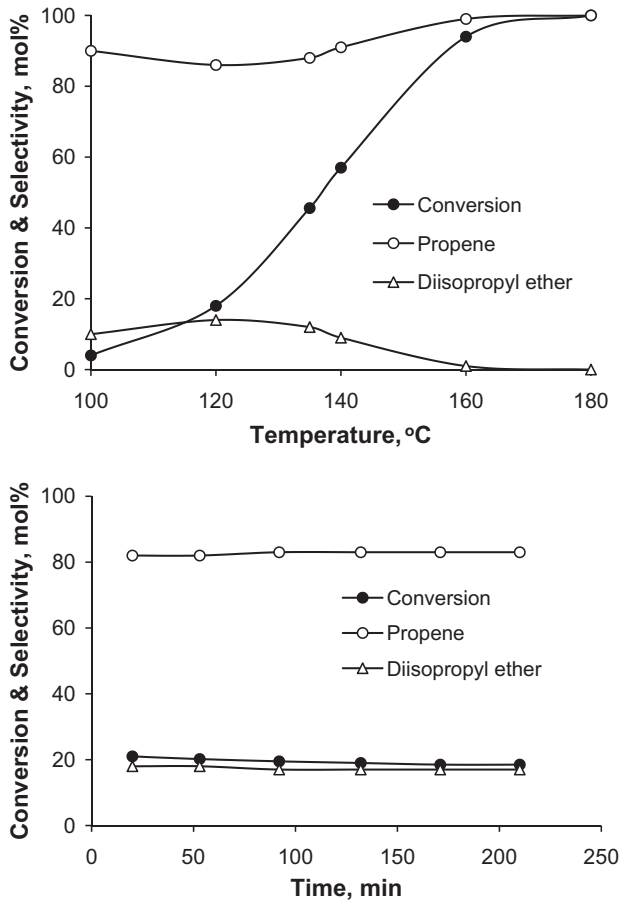

Fig. 8. Isopropanol dehydration over 15%$H_3PW_{12}O_{40}/TiO_2$-500 at isopropanol partial pressure of 5.52 kPa: light-off test (top) and isothermal test at 120 °C (bottom).

Catalyst activities under isothermal conditions are represented by isopropanol conversions at 120 °C (Table 3). These closely follow the corresponding values of T_{50}. Table 3 displays the turnover frequency (TOF) per proton site for our catalysts at 120 °C, which was calculated from the corresponding values of isopropanol conversion. The number of proton sites available for reaction was worked out as follows. For supported HPA and $Cs_2HPW_{12}O_{40}$, all protons were assumed to be equally available for reaction due to a sub-monolayer surface coverage. For bulk $Cs_{2.5}H_{0.5}PW_{12}O_{40}$, which has been suggested to catalyse isopropanol dehydration via the surface type mechanism [1,2], only surface protons were taken into account. Their number was calculated assuming a Keggin unit cross section of 144 $Å^2$ [1,2] and a surface area of 111 m^2/g for the fresh catalyst (Table 1). The surface area did not change after reaction at 120 °C, which is not surprising since the catalyst had been pre-treated at 300 °C, and no coke formation after reaction was observed. The TOF values thus obtained should be regarded as an approximation. The true values may be higher because the number of accessible proton sites on the surface could be smaller than the stoichiometric number of protons used in our calculations. Less clear was the situation with the bulk $H_3PW_{12}O_{40}$, which has been suggested to catalyse isopropanol dehydration *via* the bulk type mechanism [1]. It seemed unlikely, however, that isopropanol molecules would penetrate deep in the bulk of HPA crystals at 120 °C. Such reaction would be almost inevitably diffusion-hindered [16], which is not consistent with the high activation energy for the dehydration over bulk HPA (Table 3). Assuming that all HPA protons were available for reaction (bulk type catalysis) gave a TOF value of 23 h^{-1}, which is obviously too small. From the HPA acid strength, this value might be expected to be higher than that for $Cs_{2.5}H_{0.5}PW_{12}O_{40}$ (430 h^{-1}). If only the surface protons were active (surface type catalysis), the TOF would increase to 3500 h^{-1}, as estimated from the above Keggin unit cross section and the surface area of 2.0 m^2/g for the fresh HPA catalyst (Table 1). It is, therefore, conceivable that only the protons in top layer(s) of solid $H_3PW_{12}O_{40}$ participated in catalysis rather than all protons in the HPA bulk.

Fig. 9 shows a relationship between the catalytic activity of HPA catalysts in isopropanol dehydration, log (TOF), and their initial enthalpy of NH_3 adsorption, ΔH_i. This is a fairly good linear plot, which becomes even better if only the catalysts calcined at 300 °C are included (Fig. 10). The point for bulk $H_3PW_{12}O_{40}$, calculated assuming the surface type catalysis, fits this plot well, which supports the suggested mechanism. This relationship shows that isopropanol dehydration and NH_3 adsorption calorimetry give consistent results regarding the acidity of HPA catalysts. Recently, similar relationship between the rate constants for 2-butanol dehydration over silica-supported HPA catalysts in the gas phase and the deprotonation energies of HPA calculated by DFT has been reported [36].

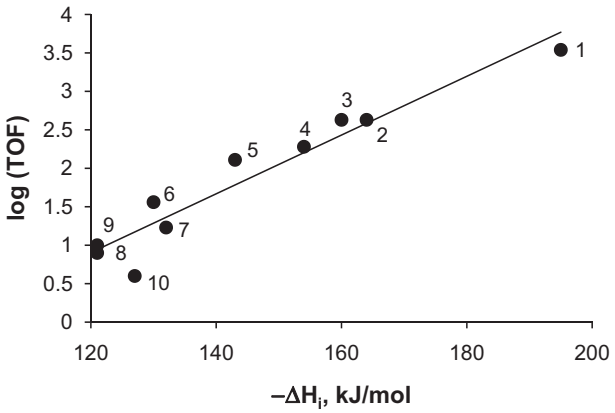

Fig. 9. Relationship between log (TOF) and ΔH_i. Point numbering corresponds to that in Table 3.

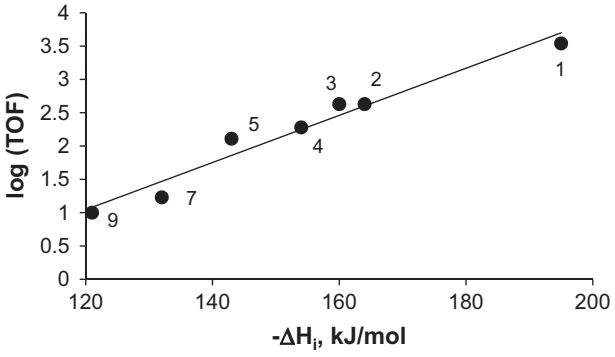

Fig. 10. Relationship between log (TOF) and ΔH_i for bulk and supported catalysts calcined at 300 °C. Point numbering corresponds to that in Table 3.

4. Conclusions

In recent years, solid acid catalysts comprising tungsten heteropoly acids, usually $H_3PW_{12}O_{40}$, supported on niobia, zirconia and titania have attracted significant interest because of their advantages for clean organic synthesis. However, only limited knowledge of their acid properties had been available. In this study, we have characterised the acid and catalytic properties of such catalysts at the gas–solid interface using ammonia adsorption calorimetry and infrared spectroscopy of adsorbed pyridine as well as gas-phase isopropanol dehydration as a test reaction. These catalysts have been compared with the well-known "standard" HPA catalysts such as bulk and silica-supported $H_3PW_{12}O_{40}$ and $Cs_{2.5}H_{0.5}PW_{12}O_{40}$. In contrast to the parent acid, $H_3PW_{12}O_{40}$, possessing strong Brønsted acid sites, the catalysts prepared by supporting $H_3PW_{12}O_{40}$ on Nb_2O_5, ZrO_2 and TiO_2 have been found to possess both Brønsted and Lewis acid sites. Their acid sites are weaker than those in $H_3PW_{12}O_{40}$ and $Cs_{2.5}H_{0.5}PW_{12}O_{40}$. The catalytic activity (turnover frequency) in isopropanol dehydration decreases in the order: $H_3PW_{12}O_{40}$ > $Cs_{2.5}H_{0.5}PW_{12}O_{40}$ > $15\%H_3PW_{12}O_{40}/SiO_2$ > $15\%H_3PW_{12}O_{40}/TiO_2$ > $15\%H_3PW_{12}O_{40}/Nb_2O_5$ > $15\%H_3PW_{12}O_{40}/ZrO_2$, which is in line with the acid strength determined by NH_3 adsorption calorimetry. From catalyst characterisation by NH_3 adsorption calorimetry, FTIR and $^{31}P\{^1H\}$ MAS NMR, it can be derived that interaction between HPA and support increases in the series of supports: SiO_2 < TiO_2 < Nb_2O_5 < ZrO_2, causing partial decomposition of HPA and decreasing the catalyst acid strength in that order. Regarding their acid strength, the $H_3PW_{12}O_{40}$ catalysts supported on Nb_2O_5, ZrO_2 and TiO_2 oxides appear to be similar to acidic zeolites. These catalysts, however, have the advantage over zeolite catalysts in better accessibility of reactant and product molecules, especially for reactions involving large organic molecules that will not fit into zeolite micropores. Development of thermally stable HPA composites possessing stronger acid sites remains a challenge for further research.

Acknowledgments

Financial support from the EPSRC, UK (Grant EP/F014686/1) and the scholarship for A. Alsalme from King Saud University, Saudi Arabia are gratefully acknowledged.

References

[1] T. Okuhara, N. Mizuno, M. Misono, Adv. Catal. 41 (1996) 113–252.
[2] I.V. Kozhevnikov, Catalysis by Polyoxometalates, Wiley & Sons, Chippenham, 2002.
[3] M. Misono, Catal. Today 100 (2005) 95–100.
[4] I.V. Kozhevnikov, J. Mol. Catal. A 305 (2009) 104–111.
[5] I.D. Dobson, Green Chem. 5 (2003) G78–G81.
[6] Y. Izumi, K. Urabe, M. Onaka, Zeolite, Clay and Heteropoly Acid in Organic Reactions, Kodansha/VCH, Tokyo, 1992.
[7] K. Okumura, K. Yamashita, M. Hirano, M. Niwa, J. Catal. 234 (2005) 300–307.
[8] K. Okumura, K. Yamashita, K. Yamada, M. Niwa, J. Catal. 245 (2007) 75–83.
[9] B.M. Devassy, S.B. Halligudi, J. Catal. 236 (2005) 313–323.
[10] B.M. Devassy, F. Lefebvre, S.B. Halligudi, J. Catal. 231 (2005) 1–10.
[11] B.M. Devassy, S.B. Halligudi, J. Mol. Catal. A 253 (2006) 8–15.
[12] D.P. Sawant, A. Vinu, F. Lefebvre, S.B. Halligudi, J. Mol. Catal. A 262 (2007) 98–108.
[13] S.M. Kumbar, G.V. Shanbhag, F. Lefebvre, S.B. Halligudi, J. Mol. Catal. A 256 (2006) 324–334.
[14] N. Bhatt, A. Patel, J. Mol. Catal. A 264 (2007) 214–219.
[15] A. Alsalme, E.F. Kozhevnikova, I.V. Kozhevnikov, Appl. Catal. A 349 (2008) 170–176.
[16] J.B. Moffat, Metal-Oxygen Clusters. The Surface and Catalytic Properties of Heteropoly Oxometalates, Kluwer, NY, 2001. p. 71.
[17] K. Srilatha, N. Lingaiah, B.L.A. Prabhavathi Devi, R.B.N. Prasad, S. Venkateswar, P.S. Sai Prasad, Appl. Catal. A 365 (2009) 28–33.
[18] E. Lopez-Salinas, J.G. Hernandez-Cortez, I. Schifter, E. Torrez-Garcia, J. Navarrete, A. Gutierrez-Carrillo, T. Lopez, P.P. Lottici, D. Bersani, Appl. Catal. A 193 (2000) 215–225.
[19] Y. Izumi, M. Ono, M. Kitagawa, M. Yoshida, K. Urabe, Micropor. Mater. 5 (1995) 255–262.
[20] E.F. Kozhevnikova, I.V. Kozhevnikov, J. Catal. 224 (2004) 164–169.
[21] P.M. Rao, P. Goldberg-Oppenheimer, S. Kababya, S. Vega, M.V. Landau, J. Mol. Catal. A 275 (2007) 214–227.
[22] N. Uekawa, T. Kudo, F. Mori, Y.J. Wu, K. Kakegawa, J. Colloid Interface Sci. 264 (2003) 378–384.
[23] F. Al-Wadaani, E.F. Kozhevnikova, I.V. Kozhevnikov, J. Catal. 257 (2008) 199–205.
[24] F. Kapteijn, J.A. Moulijn, in: G. Ertl, H. Knözinger, F. Schüth, J. Weitkamp (Eds.), Handbook of Heterogeneous Catalysis, vol. 4, Wiley-VCH, 2008, p. 2028.
[25] T. Okuhara, H. Watanabe, T. Nishimura, K. Inumaru, M. Misono, Chem. Mater. 12 (2000) 2230–2238.
[26] K. Tanabe, M. Misono, Y. Ono, H. Hattori (Eds.), New Solid Acids and Bases: Their Catalytic Properties, Kodansha, Tokyo, 1989.
[27] H. Knözinger, in: G. Ertl, H. Knözinger, F. Schüth, J. Weitkamp (Eds.), Handbook of Heterogeneous Catalysis, vol. 2, Wiley-VCH, 2008, p. 1154.
[28] F.C. Jentoft, in: G. Ertl, H. Knözinger, F. Schüth, J. Weitkamp (Eds.), Handbook of Heterogeneous Catalysis, vol. 1, Wiley-VCH, 2008, p. 263.
[29] I.V. Kozhevnikov, Chem. Rev. 98 (1998) 171–198.
[30] T. Okuhara, Chem. Rev. 102 (2002) 3641–3666.
[31] M. Brandle, J. Sauer, J. Am. Chem. Soc. 120 (1998) 1556–1570.
[32] M.T. Pope, Heteropoly and Isopoly Oxometalates, Springer, Berlin, 1983. p. 66.
[33] I.V. Kozhevnikov, K.R. Kloetstra, A. Sinnema, H.W. Zandbergen, H. Van Bekkum, J. Mol. Catal. A 114 (1996) 287.
[34] A. Gervasini, J. Fenyvesi, A. Auroux, Catal. Lett. 43 (1997) 219–228.
[35] L.R. Pizzio, C.V. Carceres, M.N. Blanco, Appl. Catal. A 167 (1998) 283–294.
[36] J. Macht, R.T. Carr, E. Iglesia, J. Catal. 264 (2009) 54–66.